Molecular Biology of the Cell
Vol. 20, 4390–4399, October 15, 2009

Pob1 Participates in the Cdc42 Regulation of Fission Yeast Actin Cytoskeleton

Sergio A. Rincón,* Yanfang Ye,† M. Antonia Villar-Tajadura,* Beatriz Santos,* Sophie G. Martin,† and Pilar Pérez*

*Instituto de Microbiología Bioquímica, Consejo Superior de Investigaciones Científicas/Departamento de Microbiología y Genética, Universidad de Salamanca, 37007 Salamanca, Spain; and †Center for Integrative Genomics, Faculty of Biology and Medicine, University of Lausanne, 1015 Lausanne, Switzerland

Submitted March 13, 2009; Revised July 27, 2009; Accepted August 18, 2009
Monitoring Editor: Daniel J. Lew

Rho GTPases regulate the actin cytoskeleton in all eukaryotes. Fission yeast Cdc42 is involved in actin cable assembly and formin For3 regulation. We isolated *cdc42-879* as a thermosensitive strain with actin cable and For3 localization defects. In a multicopy suppressor screening, we identified *pob1*$^+$ as suppressor of *cdc42-879* thermosensitivity. Pob1 overexpression also partially restores actin cables and localization of For3 in the mutant strain. Pob1 interacts with Cdc42 and this GTPase regulates Pob1 localization and/or stability. The C-terminal pleckstrin homology (PH) domain of Pob1 is required for Cdc42 binding. Pob1 also binds to For3 through its N-terminal sterile alpha motif (SAM) domain and contributes to the formin localization at the cell tips. The previously described *pob1-664* mutant strain (Mol. Biol. Cell. *10*, 2745–2757, 1999), which carries a mutation in the PH domain, as well as *pob1* mutant strains in which Pob1 lacks the N-terminal region (*pob1ΔN*) or the SAM domain (*pob1ΔSAM*), have cytoskeletal defects similar to that of *cdc42-879* cells. Expression of constitutively active For3DAD* partially restores actin organization in *cdc42-879*, *pob1-664*, *pob1ΔN*, and *pob1ΔSAM*. Therefore, we propose that Pob1 is required for For3 localization to the tips and facilitates Cdc42-mediated relief of For3 autoinhibition to stimulate actin cable formation.

INTRODUCTION

The shape and size of cells is achieved through a strict control of polarized cell growth, which requires regulation of actin organization, addition of new membranes to the zones of active growth, and, in fungal and plant cells, biosynthesis of the cell wall. These processes must be tightly coordinated temporally and spatially to permit the correct growth position in each moment of the cell cycle (Hayles and Nurse, 2001).

Rho GTPases are key molecules in polarized growth regulation, which integrate signals from both the cell cycle and the extracellular environment (Hall, 2005; Park and Bi, 2007). These proteins act as molecular switches, inactive when bound to guanosine diphosphate (GDP) and active when bound to guanosine triphosphate (GTP). GTPase activation proteins (GAPs) stimulate the intrinsic GTPase activity of the Rho proteins, leading to their inactivation; by contrast, Guanine nucleotide exchange factor (GEF) proteins promote the GDP-to-GTP exchange, thereby activating Rho proteins. Rho GTPases directly regulate the actin and microtubule cytoskeleton organization (Ridley, 2006), participate in the secretory pathway control (Brennwald and Rossi, 2007), and regulate fungal cell wall biosynthesis (Levin, 2005). To coordinate all these processes, GTP-bound Rho GTPases interact with and stimulate the activity of a variety of effector proteins.

The Rho-family GTPase Cdc42 plays a central role in the establishment of polarized cell growth through interaction with multiple effector proteins (Cerione, 2004; Etienne-Manneville, 2004). Cdc42 interacts with many proteins such as: p21-activated kinases (PAKs), which participate in actin organization (Zhao and Manser, 2005); Wiskott–Aldrich syndrome protein, which stimulates the formation of actin structures through the activation of the Arp2/3 complex (Takenawa and Suetsugu, 2007); the exocyst complex, necessary for tethering secretory vesicles to the plasma membrane (Wu *et al*., 2008); and formins, which nucleate linear actin filaments (Faix and Grosse, 2006).

Fission yeast Cdc42 is an essential protein that has been implicated in the regulation of the cell shape and growth (Miller and Johnson, 1994). It interacts with the PAKs, Shk1 and Shk2 (Yang *et al*., 1998; Chang *et al*., 1999), and it is the main Rho GTPase required for actin cable assembly (Martin *et al*., 2007). Actin cables are important structures that contribute to polarized cell growth, serving as tracks for delivery of secretory vesicles to cell tips. In *Schizosaccharomyces pombe* interphase cells the assembly of these structures depends on the formin For3, which localizes to cell tips (Feierbach and Chang, 2001). Surprisingly, For3 is not essential for cell viability, though *for3Δ* cells lack actin cables detectable by phalloidin staining. Similar to other formins, For3 is controlled by an autoinhibitory interaction between the N-terminal Dia inhibitory domain (DID) with the C-terminal Dia autoregulatory domain (DAD) (Goode and Eck, 2007). The proper localization of For3 depends on relief of this autoinhibition (Martin *et al*., 2007), and so far the only proteins involved in this process are the actin-interacting protein Bud6 and the Rho GTPase Cdc42 (Martin *et al*., 2007).

We had previously isolated several *cdc42-ts* mutant strains; screening them for multicopy suppressors we found Pob1, an essential protein implicated previously in polarized

This article was published online ahead of print in *MBC in Press* (http://www.molbiolcell.org/cgi/doi/10.1091/mbc.E09–03–0207) on August 26, 2009.

Address correspondence to: Pilar Pérez (piper@usal.es).

cell growth and cell septation (Toya *et al*., 1999). Overproduction of Pob1 partially suppresses the actin defects observed in the *cdc42-ts* mutant *cdc42-879*. Here, we describe the interactions among Cdc42, For3, and Pob1 and suggest that Pob1 contributes to relief of For3 autoinhibition.

MATERIALS AND METHODS

Strains, Growth Conditions, and Genetic Methods

Standard *S. pombe* media and genetic manipulations were used (Moreno *et al*., 1991). All the strains used were isogenic to wild-type strains *972* h^- and *975* h^+, and they are described in Supplemental Table 1. The strains were constructed by either tetrad dissection or random spore germination method. Cells were usually grown in either rich medium (YES) or minimal medium (EMM) with appropriate supplements. *Escherichia coli* DH5α was used as host for propagation of plasmids. Cells were grown in Luria-Bertani medium supplemented with 50 μg/ml ampicillin when needed. Solid media contained 2% agar.

Recombinant DNA Methods

All DNA manipulations were carried out by established methods. Enzymes were used according to the recommendations of the suppliers. *S. pombe* was transformed by the lithium acetate method (Ito *et al*., 1983). The *nmt* promoter-containing vectors pREP3X, pREP4X, and pREP1-GST (Forsburg, 1993) were used for the overexpression of *cdc42*$^+$, *gef1*$^+$, *scd1*$^+$, *shk1*$^+$, *shk2*$^+$, and *pob1*$^+$. For the multicopy expression of *pob1*$^+$ under the control of its own promoter, an EcoRI fragment of 4.1 kb containing *pob1*$^+$ open reading frame (ORF) and ~1 kb of its promoter and terminator was subcloned into pAU-KS or pAL-KS vectors. For the two-hybrid analysis, the *pob1*$^+$ ORF or different *pob1*$^+$ fragments were cloned into the NdeI-XmaI sites of pAS2. *cdc42*$^+$ ORF excluding the 3′ region codifying the prenylatable domain of Cdc42 was cloned into the NcoI-XmaI sites of pACT2. For3 two-hybrid plasmids containing *for3N* (1–702) and *for3C* (630–1461) were as described previously (Martin *et al*., 2005). *Saccharomyces cerevisiae* Y190 (*MATa gal4 gal80 his3 trp1-901 ura3-52 leu2-3,-112 URA3*::*GAL-<lacZ*, *lys2*::*GAL (UAS)-<HIS3 cyh*r) were transformed and grown on plates without leucine, tryptophan, and histidine and supplemented with 40 mM 3-aminotriazole. β-Galactosidase activity was analyzed in the transformant colonies as described previously (Coll *et al*., 2003).

Error-prone PCR for obtaining *cdc*42 ORF mutants was performed as described previously (Martin *et al*., 2007). *cdc42-879* strain identification and isolation were carried out as described previously (Martin *et al*., 2007). Screening for *cdc42-879* multicopy suppressors was performed using a *S. pombe* genomic library (pURSP1; American Type Culture Collection, Manassas, VA) to transform the mutant strain. Transformant clones were selected at 36°C; the plasmid was recovered, and its DNA insert was sequenced. To substitute the endogenous *pob1*$^+$ ORF for the region coding for Pob1ΔN (amino acids 314–871), a cassette including 0.7 kb of *pob1*$^+$ promoter, the hemagglutinin (HA) epitope coding sequence fused in frame to the *pob1* fragment, the *ura4*$^+$ selection marker, and 0.5 kb of *pob1*$^+$ terminator was constructed in a KS BlueScript vector. Subsequently, this cassette was cut with XhoI-NotI, purified, and used to transform an *h*$^+$ *leu1-32 ura4D-18* (PPG103) strain. Stable haploid transformants were selected and screened by polymerase chain reaction (PCR) for the appropriate gene replacement. A genomic version of *pob1*$^+$ with the green fluorescent protein (GFP), Cherry, or the HA epitope coding sequences fused to the ORF 5′ end was generated using different cassettes generated as described above. A genomic version of *pob1*$^+$ with the Myc epitope coding sequence fused to the 3′ end of the ORF was generated as described previously (Bähler *et al*., 1998).

Glutathione-Sepharose (GS) Pull-Down and Immunoprecipitation

Extracts from 5×10^8 cells expressing the different tagged proteins were obtained as described previously (Arellano *et al*., 1997) by using 200 μl of lysis buffer. For the analysis of Cdc42–Pob1 interaction the lysis buffer contained 50 mM Tris-HCl, pH 7.5, 5 mM EDTA, 137 mM NaCl, 0.5% NP-40, and Protease Inhibitor Cocktail (Sigma-Aldrich, St. Louis, MO); and for the analysis of For3–Pob1 interaction, it contained 50 mM HEPES, pH 7.5, 2 mM EDTA, 130 mM NaCl, 20 mM KCl, 1 mM $MgCl_2$, 1% NP-40, and Protease Inhibitor Cocktail. Cell extracts (2–3 mg of total protein) were incubated with GS beads or with the corresponding antibody and protein A-Sepharose beads for 2–4 h at 4°C. The beads were washed four times with lysis buffer and resuspended in sample buffer. Proteins were separated by SDS-polyacrylamide gel electrophoresis (PAGE), transferred to Immobilon-P membranes (Millipore, Billerica, MA), and blotted to detect the GFP-, glutathione transferase (GST)-, HA- or Myc-fused epitopes with the corresponding antibodies and the enhanced chemiluminescence detection kit (GE Healthcare, Little Chalfont, Buckinghamshire, United Kingdom). Western-blot analysis of cell extracts (50 μg total protein) was performed to determine the total amount of tagged protein.

In Vivo Analysis of Cdc42 Activity

The expression vector pGEX-Cdc42/Rac interactive binding (CRIB) (Manser *et al*., 1998) was used to transform *E. coli* and produce GST fused to the mammalian Pak2 binding domain for Cdc42. The fusion protein was produced according to the manufacturer's instructions and immobilized on GS beads. The amount of GTP-bound Cdc42 was determined using a pull-down assay as described previously (Coll *et al*., 2003). In brief, extracts from wild-type, *cdc42-879*, *pob1-664*, or wild-type overexpressing *pob1*$^+$ strains carrying integrated *HA-cdc42*$^+$ were obtained as described previously (Arellano *et al*., 1997), by using 500 μl of lysis buffer (50 mM Tris, pH 7.5, 20 mM NaCl, 0.5% NP-40, 10% glycerol, 0.1 mM dithiothreitol, 1 mM NaF, and 2 mM Cl_2Mg, containing 100 μM *p*-aminophenyl methanesulfonyl fluoride, leupeptin, and aprotinin). Cell extracts (2 mg of total protein) were incubated with 10 μg of GST–CRIB protein coupled to GS beads for 2 h, washed four times, and blotted with anti-HA monoclonal antibody (mAb). Total HA-Cdc42 levels in whole-cell extracts (30 μg of total protein) were monitored by Western blot.

Microscopy Techniques

For calcofluor white staining of *S. pombe* cell wall and septum, exponentially growing cells were harvested, washed, and resuspended in a calcofluor solution (0.1 mg/ml) for 5 min at room temperature. After washing with water, cells were observed in a microscope with the corresponding UV filter. Actin staining was performed by using AlexaFluor 488-phalloidin. HA-Cdc42 immunolocalization was performed in exponentially growing cells fixed in 16% ultrapure formaldehyde and stained using anti-HA mAb as described previously (Martin *et al*., 2007). Cell samples were observed using a DMXRA microscope (Leica Microsystems, Deerfield, IL) equipped for Nomarski optics and epifluorescence, and photographed with an Orca-ER C4742-80 camera (Hamamatsu, Bridgewater, NJ). Actin staining was analyzed using an IX71 microscope (Olympus , Tokyo, Japan) equipped with a personal Delta Vision system and a CoolSNAP HQ2 monochrome camera (Photometrics, Tucson, AZ). Stacks of six *z*-series sections were acquired at 0.4-μm intervals. Images were analyzed using deconvolution and maximum two-dimensional (2D) projections of *z*-series. For experiments involving for3DAD*, actin stainings were performed as described previously (Martin *et al*., 2007), and both actin and For3 localization were imaged on a DMI4000B inverted microscope (Leica Microsystems) equipped with a HCX PL APO 100×/1.46 numerical aperture oil objective and an UltraView spinning disk confocal system (PerkinElmer Life and Analytical Sciences, Boston, MA) (including a Yokagawa CSU22 real-time confocal scanning head, an argon/krypton laser, and a cooled 14-bit frame transfer EMCCD C9100-50 camera) (Martin and Berthelot-Grosjean, 2009). Stacks of z-series confocal sections were acquired at 0.3-μm intervals with the UltraView software, and images were rendered by 2D maximal-intensity projection.

RESULTS

cdc42-879 Is a Thermosensitive Strain That Shows Actin Cable Defects

To find new Cdc42 effectors in *S. pombe*, we searched for suppressors of a *cdc42* thermosensitive mutant strain, termed *cdc42-879*, which was obtained by degenerate PCR, as described previously (Martin *et al*., 2007). This strain showed a severe growth defect at 36°C (Figure 1A). In addition, it displayed aberrant morphology even at permissive temperature with a variety of cell shapes, namely, pear-like cells, lemon-shaped cells, round cells, and very small cells due to asymmetric septum positioning (Figure 1B). Approximately 15% of the cells grown at 28°C showed cell lysis and >50% displayed monopolar growth (compared with 22% of wild-type cells). At septation, *cdc42-879* cells were shorter (10.81 ± 1.64 μm, n = 85) and wider (4.64 ± 0.83 μm, n = 85) than wild-type cells (13.56 ± 0.91 μm, n = 68; 3.64 ± 0.21 μm, n = 51) grown in the same conditions. When mutant cells were transferred to medium at 36°C, they stopped dividing after 3 h and became ovoid (Figure 1B).

To understand the reasons behind the phenotype of *cdc42-879* cells, we analyzed whether this mutation caused changes in Cdc42 levels, localization, or activity. Total levels of Cdc42, as detected by Western blot, were similar in wild-type strain and *cdc42-879* strains, ruling out the possibility that this strain might have a defect in Cdc42 stability at 36°C (Figure 1C).

Cdc42 localizes to the growing poles and to the division area (Merla and Johnson 2000). HA-Cdc42-879 localization

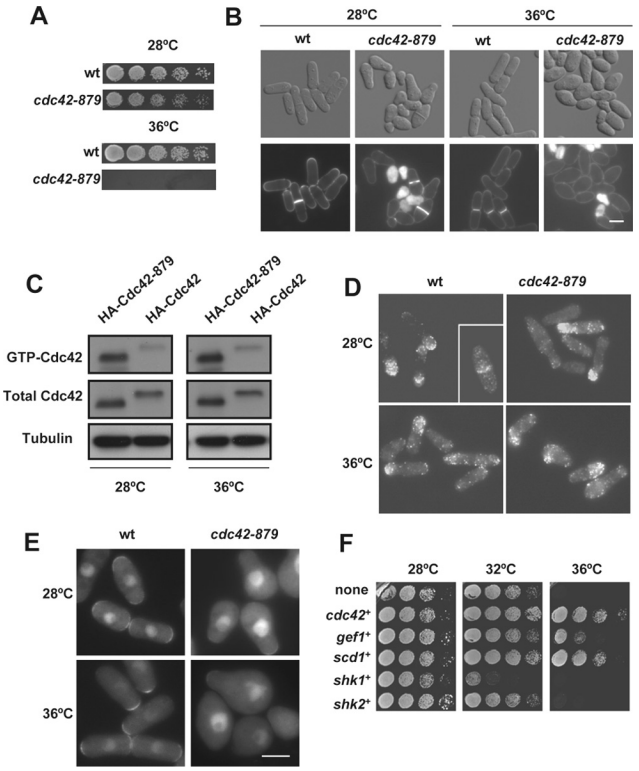

Figure 1. Morphological defects of *S. pombe cdc42-879* strain. (A) Growth of wild-type (wt) and *cdc42-879* cells spotted at one-fourth dilution in YES medium and incubated at 28 or 36°C for 3 d. (B) Differential interference contrast (DIC) and fluorescence images of wt and *cdc42-879* cells stained with calcofluor. Cells were grown at 28 or 36°C for 5 h. Bar, 5 μm. (C) Levels of GTP-bound Cdc42 in *cdc42-879* cells. Extracts from wild-type and *cdc42-879* cells grown at 28°C and transferred at 28 or 36°C for 3 h were precipitated with GST-CRIB and blotted with anti-HA antibodies (top). Total HA-Cdc42 in cell lysates was visualized by Western blot. Tubulin was used as loading control. (D) Immunofluorescence of HA-Cdc42 (wt) and HA-Cdc42–879 with anti-HA antibody. Both wild-type and mutant *cdc42-879* cells were grown at 28°C and transferred at 36°C for 3 h. (E) Localization of GTP-bound Cdc42 by using wt and mutant *cdc42-879* cells carrying integrated Gic2 CRIB-GFP. Cells were grown at 28°C and transferred at 36°C for 3 h. (F) Rescue of *cdc42-879* thermosensitive growth defect by expression of Cdc42 pathway proteins. *cdc42-879* cells were transformed with the expression plasmid pREP81X carrying either no insert, *cdc42*$^+$, the coding genes for the GEFs *gef1*$^+$ and *scd1*$^+$, and the coding genes for the PAKs *shk1*$^+$ and *shk2*$^+$. Cells were grown on minimal media plates for 3 d at the indicated temperatures.

was similar to that of wild-type Cdc42 as observed by immunofluorescence of fixed cells grown at either 28 or 36°C (Figure 1D). We could not observe Cdc42-879 in live cells because we were unable to tag the protein with enhanced GFP in the N-terminal region, probably because the resulting protein is nonfunctional.

Analysis of the total levels of active GTP-Cdc42 in the *cdc42-879* mutant strain by pull-down using GST-CRIB from mammalian Pak2 (Manser *et al*., 1998) showed no decrease with respect to the levels of wild-type cells. On the contrary, a larger proportion of Cdc42-879 seemed to be GTP associated (Figure 1C). However, when we investigated the localization of active Cdc42 by imaging the Gic2 CRIB domain tagged with GFP, which binds to GTP-bound Cdc42 in live cells (Tatebe *et al*., 2008), we discovered that the intensity of the CRIB-GFP signal was much weaker at the growing poles and the septum region of *cdc42-879* cells than in wild-type cells (Figure 1E). Together, these results suggest that *cdc42-879* aberrant cell shape and thermosensitivity are not due to mislocalization of Cdc42 or to a global decrease in active Cdc42. Instead, they might be caused by a decrease in the level of GTP-Cdc42 in the areas of growth, as shown in Figure 1E, or by the lack of signaling to a specific effector protein.

Overexpression of *cdc42*$^+$ or of its GEFs, in particular *scd1*$^+$, which localizes to the growth areas (Hirota *et al*., 2003), restored the ability of *cdc42-879* cells to grow at 36°C (Figure 1F), suggesting that a lack of localized GTP-Cdc42 might cause the *cdc42-879* phenotype. In contrast, overexpression of *shk1*$^+$ or *shk2*$^+$ genes, coding for the *S. pombe* PAK kinases, which are the two main Cdc42 effector proteins in *S. pombe*, did not suppress *cdc42-879* thermosensitivity. Indeed *shk1*$^+$ overexpression was rather toxic in *cdc42-879* cells, which barely grew at 32°C (Figure 1F). These results suggest that the thermosensitivity of this strain is not due to a defect in the PAK signaling pathways.

Because Cdc42 has been implicated in the organization of the actin cytoskeleton, we performed actin staining in *cdc42-879* strain. The mutant cells have very weak and short actin cables as well as depolarized actin patches (Figure 2A). To corroborate the actin cable defects, localization of Myo52, a type V myosin, and the formin For3 were examined. In wild-type cells, Myo52, which carries secretory vesicles along the actin cables, localizes to the growing poles and to the division area during cytokinesis (Motegi *et al*., 2001). However, in *cdc42-879* cells, Myo52-GFP was barely detectable at the cell poles, displaying a punctuate localization in the cytoplasm (Figure 2B). Similarly, For3-3GFP localization was reduced in *cdc42-879* mutant cells compared with wild-type cells even at permissive temperature (Figure 2C). These results show that *cdc42-879* cells have a defect in actin cable organization similar to that observed in *cdc42-1625* mutant strain (Martin *et al*., 2007).

Sequence analysis of the *cdc42*$^+$ ORF in the *cdc42-879* mutant strain showed that it contains two point mutations that generate two amino acid changes, D76G and L160S, in the protein. It is noteworthy that the latter mutation is very close to that harbored by Cdc42-1625 protein A159V (Martin *et al*., 2007). To know the contribution of the two mutations to the phenotype of the *cdc42-879* cells, we generated a *cdc42D76G* allele and a *cdc42L160S* allele and used them to replace the endogenous wild-type *cdc42*$^+$. Although *cdc42D76G* cells grew at a rate similar to that of a wild-type strain at 36°C, *cdc42L160S* cells were unable to grow at this temperature (Supplemental Figure 1A). In addition, *cdc42D76G* cells were shorter and wider than wild-type cells, whereas *cdc42L160S* cells had aberrant morphology similar to *cdc42-879* cells (Supplemental Figure 1B). *cdc42L160S* cells showed defects in actin cable organization, Myo52-GFP, and For3-3GFP localization similar to those in *cdc42-879* cells (Supplemental Figure 1, C–E). In contrast, *cdc42D76G* cells had no major actin defects. Together, these results indicate that *L160S* mutation is largely responsible for the *cdc42-879* thermosensitivity and actin cable defects.

Pob1 Is a Multicopy Suppressor of cdc42-879 Thermosensitivity That Restores Actin Cable Formation and For3 Localization

The mutant strains *cdc42-879* and *cdc42L160S* showed similar defects in actin organization and morphology. Moreover, the two mutant strains were thermosensitive and were not suppressed by overproduction of either Shk1 or Shk2. To identify new effectors of Cdc42 we searched for multicopy suppressors of *cdc42-879*. We used the *cdc42-879* allele be-

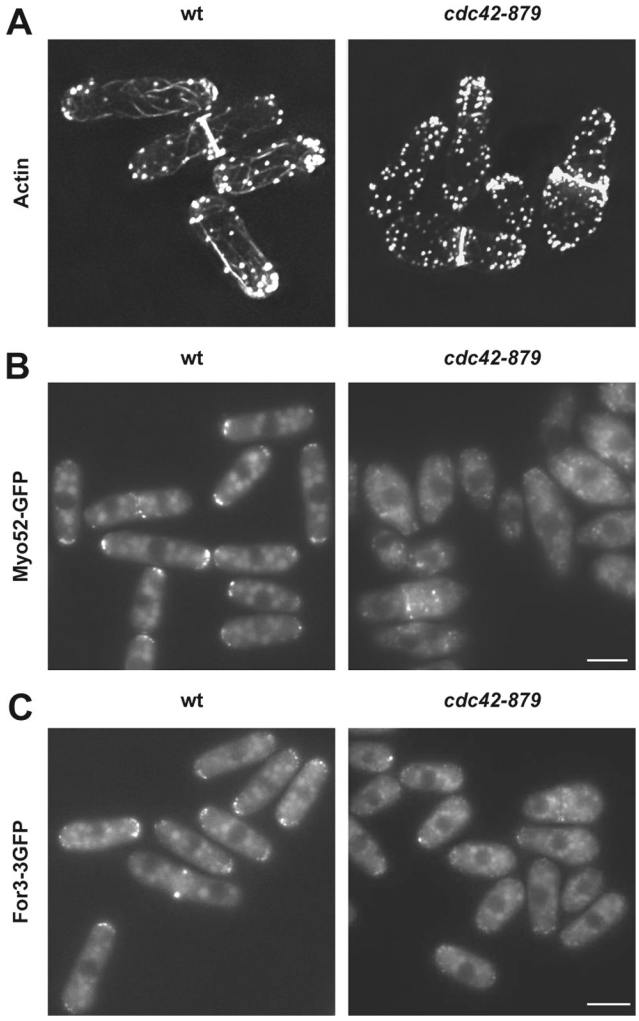

Figure 2. Actin defects of *cdc42-879* strain. (A) Actin staining of wild-type (wt) and *cdc42-879* strains grown at 28°C by using AlexaFluor 488-phalloidin. Fluorescence images of Myo52-GFP (B) and For3-3GFP (C) in wt and *cdc42-879* cells grown at 28°C.

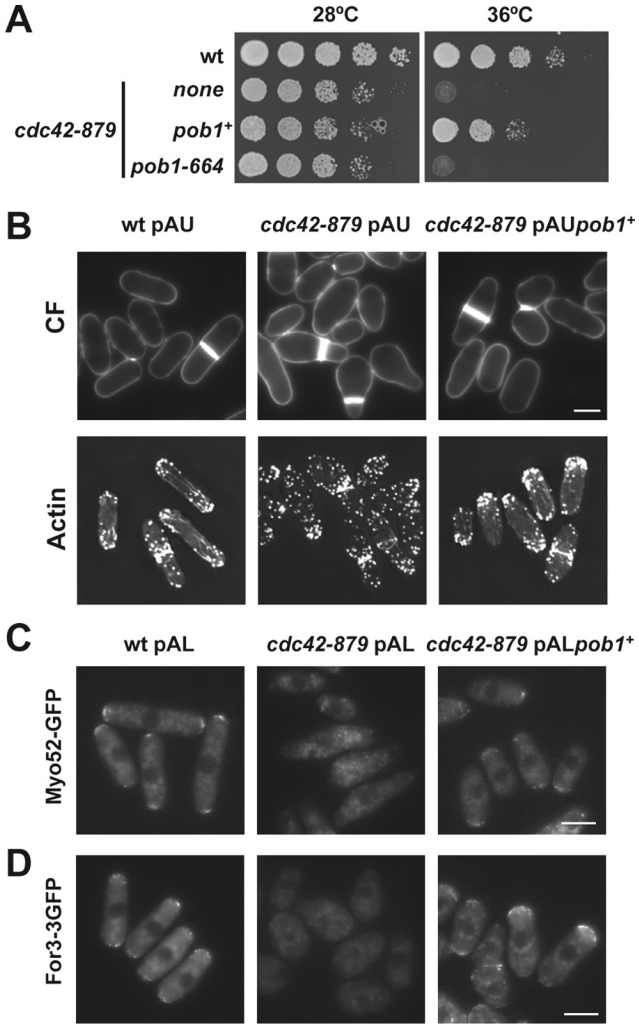

Figure 3. Pob1 is a *cdc42-879* suppressor. (A) Growth of wild-type (wt) and *cdc42-879* transformed with the plasmid pREP42HA empty or carrying *pob1*$^+$ or *pob1-664* as inserts. Cells were spotted at one-fourth dilution in minimal medium and incubated at 28 or 36°C during 3 d. (B) Fluorescence images of wt and *cdc42-879* cells transformed with the plasmid pAU or pAU-*pob1*$^+$. Cells grown at 28°C and shifted to 36°C for 5 h were stained with calcofluor (CF) (top) or AlexaFluor 488-phalloidin (bottom). Fluorescence images of Myo52-GFP (C) or For3-3GFP (D) in the same strains grown at 28°C. Bar, 5 μm.

cause it has a more severe thermosensitive phenotype in minimal medium than *cdc42L160S* cells. *S. pombe* genomic DNA library pURSP1 was used to transform *cdc42-879* cells and transformant clones were selected at 36°C. One of these clones contained a plasmid that included over 9 kb of the cosmid SPBC1289 (nucleotides 4120–13622). This fragment contained several ORFs including *pob1*$^+$, coding for an essential protein involved in cell morphogenesis. Pob1 is homologous to Boi1 and Boi2 from *S. cerevisiae* (Toya *et al.*, 1999) and has 871 amino acids, including a Scr homology (SH)3 domain (residues 9–60), a sterile alpha motif (SAM) domain (residues 248–312), and a pleckstrin homology (PH) domain (residues 703–806). *pob1-664*, a thermosensitive mutant strain, becomes misshapen at 36°C (Toya *et al.*, 1999), displaying lemon-shaped cells similar to *cdc42-879* cells. Overexpression of *pob1*$^+$ partially suppressed *cdc42-879* thermosensitivity (Figure 3A). In contrast, overexpression of *pob1-664* did not restore the ability of *cdc42-879* cells to grow at 36°C (Figure 3A). Multicopy expression of *pob1*$^+$ under its endogenous promoter also partially suppressed *cdc42-879* thermosensitivity. The morphology of *cdc42-879* cells overexpressing *pob1*$^+$ was similar to that of wild-type cells, although they were more irregular, slightly shorter, and wider (Figure 3B). These results suggest that *cdc42-879* mutant might have other defects besides those suppressed by *pob1*$^+$ overexpression.

Because the multicopy expression of *pob1*$^+$ had an important effect on the thermosensitivity and the morphology of *cdc42-879* cells, we analyzed the actin cytoskeleton of these cells by phalloidin staining. Multicopy expression of *pob1*$^+$ in *cdc42-879* cells restored polarized actin patches and longer and stronger actin cables as compared with *cdc42-879* cells, although they seemed to be slightly more disorganized than in wild-type cells (Figure 3B). In agreement with the observation that actin cables were restored in *cdc42-879* cells overexpressing *pob1*$^+$, Myo52-GFP and For3-3GFP localized properly to the poles of these cells (Figure 3, C and D, respectively). Together, these results suggest that Pob1 may participate in Cdc42 signaling to activate actin cable formation and to localize For3.

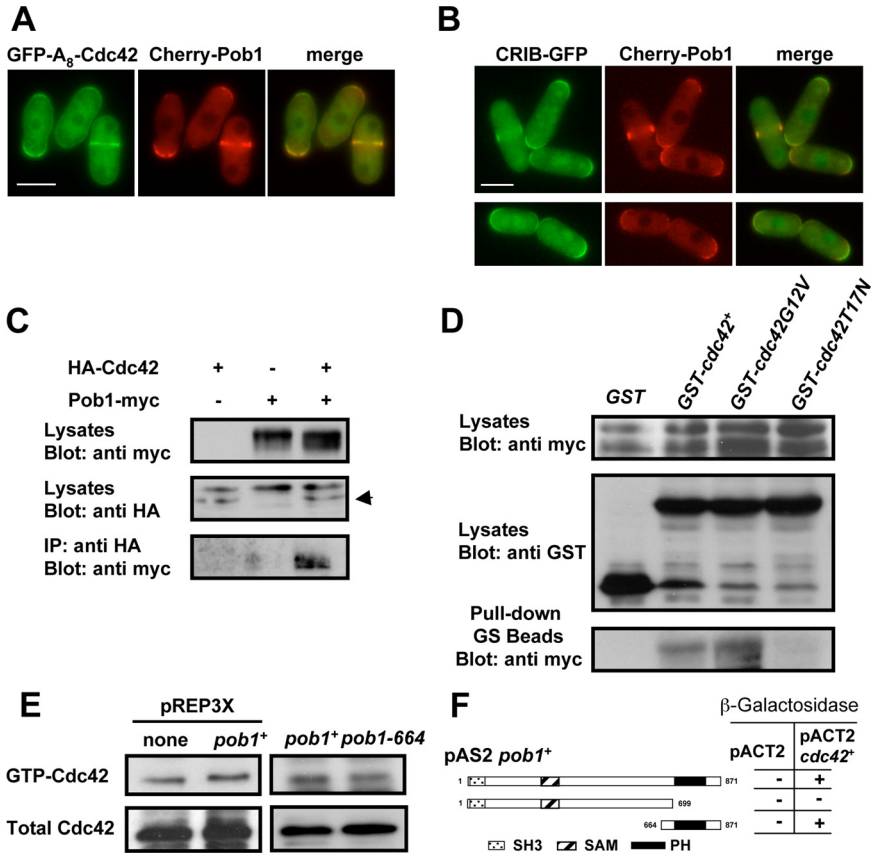

Figure 4. Pob1 physically interacts with Cdc42 in a GTP-dependent manner. (A) Cells containing GFP-A_8-Cdc42 and Cherry-Pob1 were grown to log phase and examined by fluorescence microscopy. (B) Cells containing CRIB-GFP and Cherry-Pob1 were grown to log phase and examined by fluorescence microscopy. (C) Extracts from cells expressing HA-Cdc42 and Pob1-Myc under their endogenous promoters were immunoprecipitated using anti-HA antibody and probed with anti-Myc antibody. Extracts were assayed for the level of HA-Cdc42 and Pob1-Myc by Western blot. Arrow points to HA-Cdc42 band. (D) Cells expressing endogenous Pob1-Myc were transformed with pREP1-*GST*, pREP1-*GSTcdc42*$^+$, pREP1-*GSTcdc42G12V*, or pREP1-*GSTcdc42T17N* and grown in the absence of thiamine for 14 h. Cell extracts were pulled down with GS beads, and the precipitates were probed with anti-Myc antibody. Expression of Pob1-Myc and GST-Cdc42 alleles was analyzed by Western blot. (E) Pob1 does not regulate the amount of GTP-bound Cdc42. Extracts from wild-type cells, cells overexpressing *pob1*$^+$, or *pob1-664* cells carrying *HA-cdc42*$^+$ incubated at 36°C for 5 h were precipitated with GST-CRIB and blotted with anti-HA antibodies (top). Total HA-Cdc42 in cell lysates was visualized by Western blot (bottom). (F) β-Galactosidase analysis of the two-hybrid interaction between Cdc42 and different fragments of Pob1. Several regions of the *pob1*$^+$ ORF were cloned into pAS2 and used as bait for *cdc42*$^+$ cloned into pACT2.

Pob1 Physically Interacts with Cdc42 in a GTP-dependent Manner

To address the relationship between Cdc42 and Pob1, we first analyzed the localization of both proteins. It had been described previously that both Cdc42 and Pob1 localized to the growing poles and to the division area (Toya *et al*., 1999; Merla and Johnson, 2000). We found that GFP-A_8-Cdc42 partially colocalized with Pob1 (Figure 4A); moreover, CRIB-GFP also colocalized with Cherry-Pob1 (Figure 4B), suggesting that Pob1 and active Cdc42 interact. To test for physical interaction, we performed coimmunoprecipitation experiments. Using strains expressing HA-Cdc42 and Pob1-Myc under the control of their endogenous promoters, we found that anti-Myc antibodies immunoprecipitated HA-Cdc42 together with Pob1-Myc (Figure 4C). To determine whether this interaction was dependent on the activation state of Cdc42, the strain expressing Pob1-Myc was transformed with pREP1-GST plasmids containing either the wild-type *cdc42*$^+$ allele, the hyperactive allele (*cdc42G12V*), or the dominant negative allele (*cdc42T17N*). Pull-down of GST using GS beads detected the highest levels of Pob1-Myc in the pull-down of extracts containing constitutively active Cdc42 (GST-Cdc42G12V). We also detected Pob1-Myc in the pull-down of GST-Cdc42 containing extracts but Pob1-Myc was hardly detected in pull-down experiments with extracts expressing the dominant negative *GST-cdc42T17N* allele (Figure 4D). These results indicate that Pob1 interacts with GTP-bound Cdc42.

There are two kinds of proteins that interact with active GTPases: effector proteins and GAPs, which negatively regulate Rho proteins. To determine the role of Pob1 regarding Cdc42, we analyzed the global levels of Cdc42-GTP in a strain overexpressing *pob1*$^+$ and in a strain containing the *pob1-664* allele incubated 5 h at 36°C (Figure 4E). There was no significant difference in the levels of Cdc42-GTP. Therefore, we conclude that Pob1 is not a GAP for Cdc42.

The region of Pob1 that interacts with Cdc42 was mapped using the two-hybrid system by cloning several regions of the *pob1*$^+$ ORF as bait in pAS2 and *cdc42*$^+$ in pACT2 (Durfee *et al*., 1993). Cdc42 interacted with the C-terminal PH-containing region of Pob1 and this interaction was abolished when the PH domain was absent (Figure 4F). These results indicate that Cdc42 interacts with the PH domain of Pob1 that has been described as essential for its function (Toya *et al*., 1999). Interestingly, in the two-hybrid assay *pob1*$^+$ not only interacted with *cdc42G12V* and *cdc42*$^+$ but also interacted with the dominant-negative *cdc42T17N* allele (data not shown). Therefore, it might not be Pob1 but other molecule sensing the activation state of Cdc42 in the complex detected by coimmunoprecipitation.

Cdc42 Regulates Pob1 Localization and/or Stability

Because *pob1*$^+$ overexpression suppressed the phenotype of *cdc42-879* and could be a target protein of Cdc42 signaling, we analyzed the localization of GFP-Pob1 to see whether this protein was altered in *cdc42-879* cells. We could only detect a faint signal of Pob1 localized to the division area of *cdc42-879* cells, whereas polar localization of Pob1 was completely abolished even at permissive temperature (Figure 5A). Overexpression of wild-type *cdc42*$^+$ in *cdc42-879* cells restored Pob1 localization to the growing areas (Figure 5A). We also analyzed the localization of Pob1 in the *cdc42D76G* and *cdc42L160S* mutant strains and found that Pob1 was localized in *cdc42D76G* as in wild-type cells, but the local-

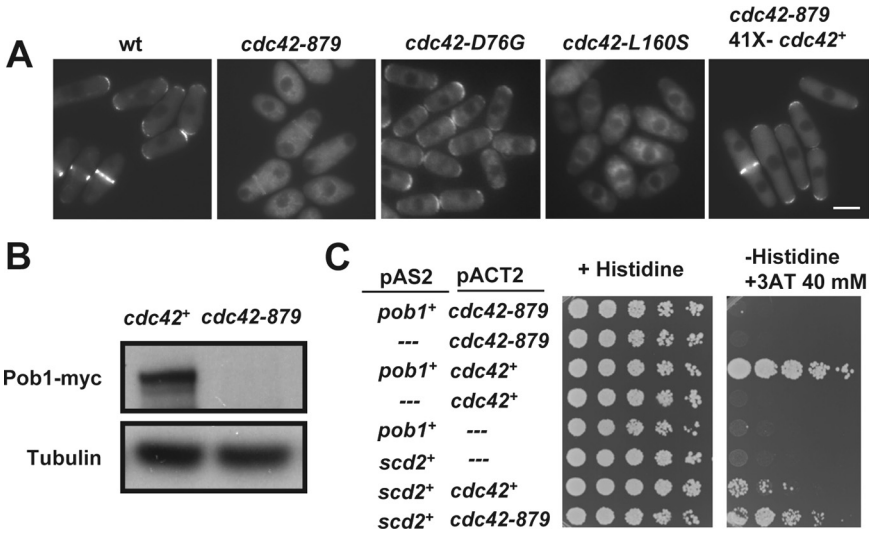

Figure 5. Cdc42 regulates Pob1 localization. (A) Localization of GFP-Pob1 in wild-type (wt), *cdc42-879*, *cdc42D76G*, *cdc42L160S*, and *cdc42-879* cells transformed with the overexpression plasmid pREP41X*cdc42*$^{+}$ grown at 28°C. (B) Total Pob1-myc in lysates from wild-type and *cdc42-879* cells grown at 28°C visualized by Western blot by using anti-myc antibody (top). Tubulin was visualized in the same extracts as loading control (bottom). (C) Two-hybrid analysis of the interaction between Pob1 or Scd2 (pAS2) with Cdc42 or Cdc42–879 (pACT2). Interaction was assessed by growth on YNB plates without histidine and supplemented with 40 mM 3-amino triazol (3-AT).

ization at the tips was abolished in *cdc42L160S* cells (Figure 5A). To see whether the lack of GFP-Pob1 signal was caused by Pob1 dispersion into the cytoplasm or by Pob1 degradation in *cdc42-879* cells, we analyzed Pob1-myc levels by Western blotting. Pob1-myc was barely detectable, suggesting that Pob1 may be unstable in *cdc42-879* (Figure 5B).

The observed Pob1 localization and/or stability defect in *cdc42-879* cells could be caused by a defective interaction of Pob1 with the Cdc42-879–mutated protein. Indeed, the mutated Cdc42-879 protein was unable to interact with Pob1 by two-hybrid analysis (Figure 5C). As a positive control, we used Scd2, a Cdc42 scaffold protein (Chang *et al.*, 1994; Endo *et al.*, 2003), that interacted with both wild-type Cdc42 and mutated Cdc42–879. These results suggest that Pob1 interaction with Cdc42 is important for its localization and/or stability.

Pob1 Binds to For3 and Might Facilitate the Cdc42-mediated Relief of Autoinhibition

Overexpression of *pob1*$^{+}$ partially suppresses the thermosensitivity and restores For3 localization in *cdc42-879*. These results led us to consider the hypothesis that Pob1 could participate in Cdc42 activation of For3. We first tested whether the *cdc42-879* actin defects may be due to a failure to activate For3. We found that expression of the constitutively active *for3DAD** allele, which blocks the autoinhibitory intramolecular interaction between For3 DID and DAD domains, improved cell shape and actin patch localization in *cdc42-879* as it did in *cdc42-1625* mutant strain (Martin *et al.*, 2007). In addition, For3DAD*-2GFP localized more efficiently than wild-type For3-3GFP in *cdc42-879* cells (Figure 6A). This suggests that, as is the case for Cdc42-1625, Cdc42-879 fails to efficiently relieve For3 autoinhibition.

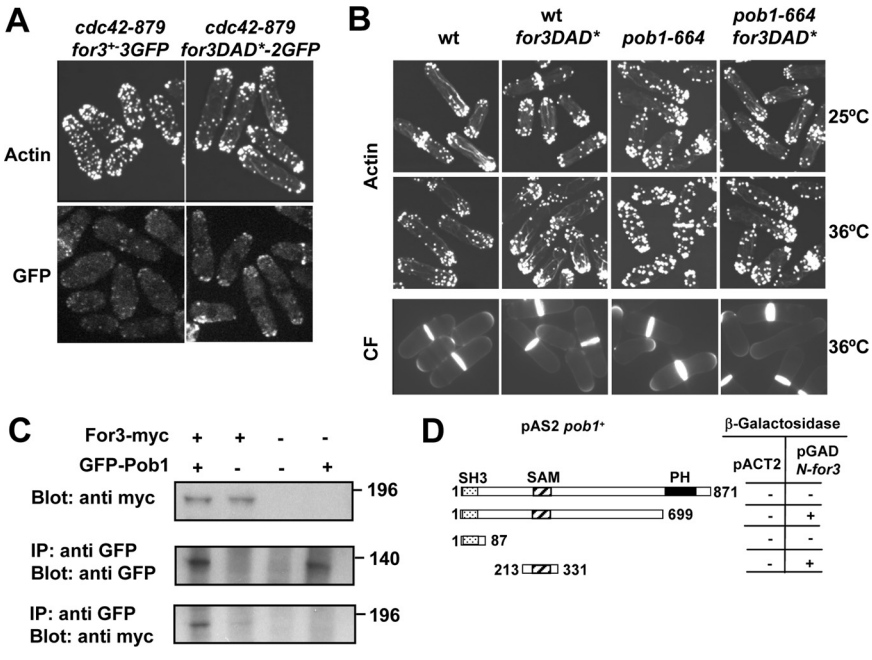

Figure 6. Pob1 binds to For3 and might facilitate the Cdc42-mediated relief of autoinhibition. (A) Actin staining of *cdc42-879* endogenously expressing *for3*$^{+}$*-3GFP* or *for3DAD*-2GFP* alleles (top). Localization of For3-3GFP or For3DAD*-2GFP in *cdc42–879* cells (bottom). (B) Actin (top and middle) and calcofluor (CF) staining (bottom) of wild-type (wt), wild-type cells expressing *for3DAD**, *pob1-664*, and *pob1-664* cells expressing *for3DAD** grown at 25 or 36°C. (C) Extracts from cells expressing GFP-Pob1 and For3-Myc under their endogenous promoters were immunoprecipitated using anti-GFP antibody and probed with anti-Myc antibody. Extracts were assayed for the level of GFP-Pob1 and For3-Myc by Western blot. (D) Two-hybrid analysis of the interaction between different fragments of Pob1 and For3. Several regions of the *pob1*$^{+}$ ORF were cloned into pAS2 and the *for3* sequence coding for the N-terminal half of For3 (amino acids 1–702), cloned into pGAD was used as bait.

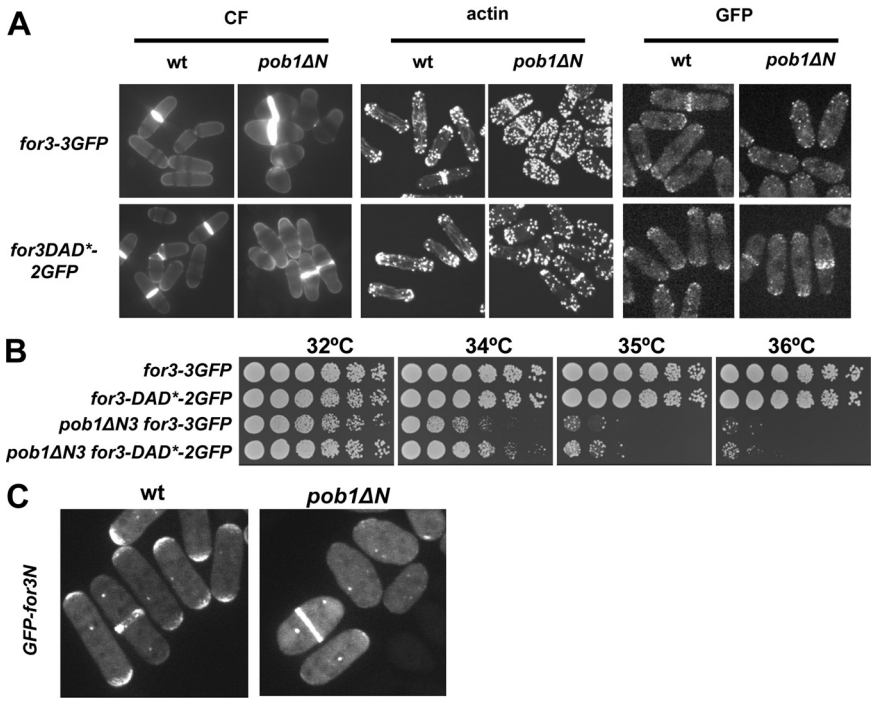

Figure 7. The N-terminal region of Pob1 is required for For3 localization. (A) Wild-type and *pob1ΔN* strains grown at 30°C in YES expressing either *for3-3GFP* or *for3DAD*-2GFP* stained with calcofluor (left) and with AlexaFluor 488-phalloidin (middle) to see the actin. Fluorescence images of For3-3GFP or For3-DAD*-2GFP in the same strains grown at 30°C in YES (right). (B) *for3DAD** expression improves the thermosensitive slow growth of *pob1ΔN* cells. Cells spotted at 1/4 dilution in YES medium and incubated at 32, 34, 35, and 36°C for 3 d. (C) Localization of GFP-For3N (including For3 amino acids 1–702) expressed from a plasmid under control of the medial-strength *nmt1* promoter in wild-type and *pob1ΔN* cells.

pob1-664 mutant cells grown at restrictive temperature (36°C) display pear-shaped and lemon-shaped morphologies similar to *cdc42-879* cells (Toya *et al*., 1999). They also showed actin cytoskeleton defects similar to *cdc42-879* cells (Figure 6B). Although at the permissive temperature of 28°C, GFP-tagged Pob1-664 localized correctly to cell ends and septum and bound Cdc42 in a two-hybrid assay (data not shown), GFP-Pob1-664 seemed to be unstable at 36°C because it could hardly be detected by fluorescence or in cell extracts (Supplemental Figure 2, B and C). To test whether *pob1-664* actin defects at 36°C were also due to defective For3 activation, we analyzed *pob1-664* cells expressing *for3DAD**. We found that these cells were longer (14.69 ± 0.90 μm) than *pob1-664* single mutant cells incubated at 36°C (13.13 ± 1.06 μm) (Figure 6B). Moreover, actin patches of *pob1-664 for3DAD** cells were better polarized than those of *pob1-664* cells and they had slightly more cables (Figure 6B). We tried to analyze For3DAD*-2GFP localization in *pob1-664* cells, but it was impossible to reach a conclusion due to imaging problems of For3-GFP at 36°C. Together, these results suggest that *pob1-664* defects are due in part to a failure to activate For3.

We next checked whether Pob1 interacts with For3 by using a strain expressing For3-myc and GFP-Pob1 from their own promoters. For3-myc was detected in anti-GFP immunoprecipitates of cell extracts containing GFP-Pob1 (Figure 6C). The regions of For3–Pob1 interaction were mapped using the two-hybrid assay. We could detect interaction of the For3 N-terminal part with the Pob1 SAM domain, and this interaction was abolished when we used as bait the whole *pob1*$^+$ ORF, including the PH domain (Figure 6D).

To test the significance of the Pob1–For3 interaction in vivo, we exchanged endogenous *pob1*$^+$ for *pob1ΔN*, which lacks the N-terminal region coding for the SH3 and SAM domains (amino acids 1–314). These cells were viable but showed slow growth phenotype that is more pronounced at high temperatures and were pear or lemon shaped. Actin cables were barely visible in these mutant cells and For3-3GFP localization was severely compromised (Figure 7A). Similar to what happens with the *pob1-664* mutant, expression of *for3DAD** improved cell morphology and actin cytoskeleton organization in *pob1ΔN* cells. In addition, For3DAD* localized better than wild-type For3 in *pob1ΔN* (Figure 7A).

We also analyzed whether the expression of *for3DAD** was able to improve the slow growth of *pob1ΔN* cells. As shown in Figure 7B, *for3DAD** partially suppresses the slow growth and thermosensitivity of *pob1ΔN* cells. To test whether activated For3DAD* improves any mutant with defective actin polarity, we analyzed its effect in *orb3-167* cells that carry a mutant allele of the kinase *nak1*$^+$ (Leonhard and Nurse, 2005). However, as shown in Supplemental Figure 3, *for3DAD** expression did not suppress the round thermosensitive phenotype of *orb3-167*, suggesting that its rescuing effects are specific to *cdc42* and *pob1* mutants.

The above-mentioned results suggest that Pob1 participates in the relief of For3 autoinhibition, which is necessary for For3 localization to cell tips.

For3 anchoring at the tips is mediated by two independent localization domains—one domain in the N terminus and one domain in the C terminus (Nakano *et al*., 2002; Martin *et al*., 2005, 2007). Although the C terminus is anchored in a Bud6-dependent manner, the anchor for the N terminus is unknown (Martin *et al*., 2007). Because Pob1 binds the N terminus of For3 (Figure 6D), we analyzed the localization of a GFP-for3N fragment (including For3 amino acids 1–702) expressed from a plasmid under control of the medial-strength *nmt1* promoter in wild-type and *pob1ΔN* cells. As shown in Figure 7C, GFP-for3N localization at cell tips is very reduced in *pob1ΔN* cells but still localizes well to the septum (and to the spindle pole body [SPB], which may be an artifact). Thus, these results indicate that the N-terminal region of Pob1 is required for the localization of For3 at cell tips. We were unable to study the localization of GFP-for3N in *pob1-664* or *cdc42-879* mutants, as GFP-for3N localization to cell tips is unstable at 36°C even in wild-type cells.

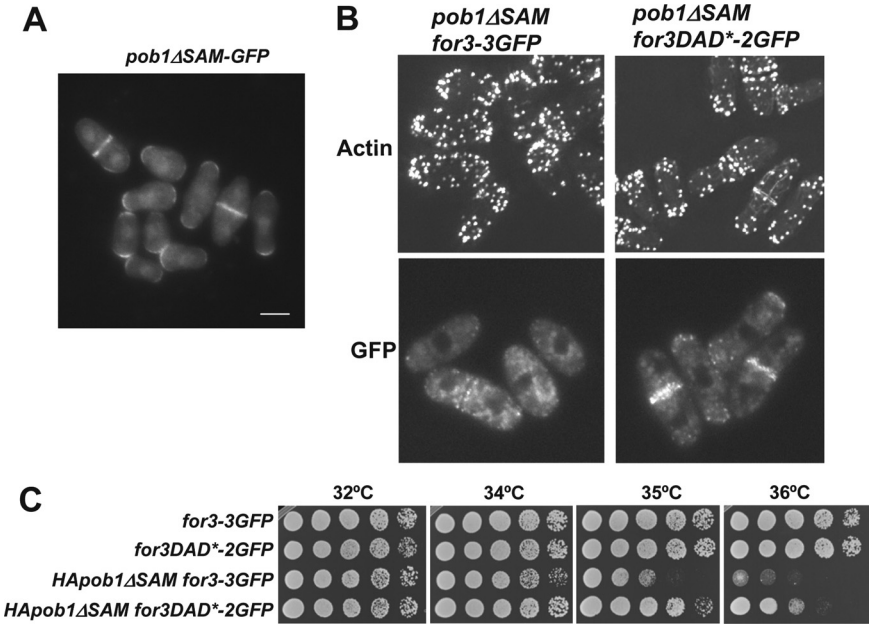

Figure 8. The SAM domain of Pob1 is required for For3 localization. (A) Fluorescent microscopy of *GFP-pob1ΔSAM*–expressing cells. Bar, 5 μm. (B) Actin staining of *pob1ΔSAM* endogenously expressing *for3*$^{+}$*-3GFP* or *for3DAD*-2GFP* alleles (top). Localization of For3-3GFP or For3DAD*-2GFP in *pob1ΔSAM* (bottom). (C) *for3DAD** expression improves the thermosensitive slow growth of *HA-pob1ΔSAM* cells. Cells spotted at one-fourth dilution in YES medium and incubated at 32, 34, 35, and 36°C for 3 d.

The N-terminal truncation of Pob1 is likely to abolish binding to other proteins in addition to For3. To characterize more closely the function of the domain involved in Pob1-For3 interaction, we made two additional deletions: *pob1ΔSH3* (lacking amino acids 1–63) and *pob1ΔSAM* (lacking amino acids 197–327). Cells carrying *pob1ΔSH3* did not have morphology defects and the actin cytoskeleton was similar to wild type (data not shown). GFP-Pob1ΔSAM was properly localized (Figure 8A). However, cells carrying this *pob1* mutant allele were pear or lemon shaped and actin cables were difficult to detect (Figure 8B). Expression of *for3DAD** improved cell morphology and actin cytoskeleton organization in these cells. Moreover, *pob1ΔSAM* cells have a growth thermosensitivity defect that was partially suppressed by *for3DAD** (Figure 8C). Both the morphology and thermosensitivity defects of *pob1ΔSAM* cells are not as pronounced as those of *pob1ΔN* cells, suggesting that the SH3 domain might collaborate in the For3 binding or might bind to other proteins that participate in Pob1 function.

DISCUSSION

Cdc42 is an essential protein controlling actin cytoskeleton organization and cell morphogenesis. Here, we describe that Pob1, the only protein of the Boi family in *S. pombe*, is a multicopy suppressor of *cdc42-879* thermosensitivity and cytoskeletal defects. We propose that Pob1 is a novel Cdc42 target that facilitates the interaction of GTP-Cdc42 with downstream effectors, including the formin For3.

Regulation of Pob1 by Cdc42

Boi proteins regulate cell growth through their interaction with Rho GTPases in several organisms. *Ashbya gossypii* Boi1/2 interacts with Rho3 to regulate polarisome localization, including the formin AgBni1 (Knechtle *et al*., 2006). In *S. cerevisiae*, it has been shown that Boi proteins also participate in bud emergence (Bender *et al*., 1996; Matsui *et al*., 1996) and are required for cell growth (McCusker *et al*., 2007). Furthermore, Boi1 has been shown to bind activated, but not dominant-negative, alleles of Cdc42 (Bender *et al*., 1996). We have shown that Pob1 preferentially binds to active Cdc42 in coimmunoprecipitation experiments, although it does not have a CRIB domain. This suggests that the Boi family of proteins may be regulated by Rho-family proteins through similar mechanisms in various species.

We have ruled out the possibility that Pob1 is regulating Cdc42 because neither the overexpression nor the mutation of *pob1*$^{+}$ causes a detectable change in the levels of active Cdc42. Localization studies indicate that Pob1 functions downstream of Cdc42, because Cdc42 regulates Pob1 localization and/or stability and not the opposite: in *cdc42-879* cells, in which Cdc42 is unable to bind to Pob1, this protein failed to localize to the cell tips and was largely degraded. When Cdc42 was overproduced in *cdc42-879* cells, the location of Pob1 to the poles was restored. We note however that Pob1 is delocalized from cell tips in *cdc42-879* or *cdc42L160S* strains even at permissive temperature, suggesting that Pob1 delocalization may not be the only reason for the thermosensitivity of these strains. By contrast, GFP-A_8-Cdc42 and GTP-Cdc42 remained localized to the tips of *pob1-664* mutant cells at 36°C (Supplemental Figure 2A), a temperature at which Pob1-664–mutated protein is unstable. Together, these results suggest that Pob1 is a novel Cdc42 target. Other examples of Rho GTPases controlling effector localization and stability have been proposed, such as Rho1 and Rho2 regulating Pck1 and Pck2 stability (Arellano *et al*., 1999; Sayers *et al*., 2000; Calonge *et al*., 2003; Villar-Tajadura *et al*., 2008).

We mapped the region of Pob1 that interacts with Cdc42 to the C-terminal PH-containing region that is essential for the function of Boi proteins (Bender *et al*., 1996; Toya *et al*., 1999). In budding yeast, mutant versions of Boi1 with changes in the PH domain still localize to mother/bud necks but not to buds (Hallett *et al*., 2002). Similarly, we have found that in *cdc42-879* cells, Pob1 localized to the division area but not to the poles, suggesting that Cdc42 binding is necessary for the cell tip location of Pob1. It is interesting that *pob1-664* thermosensitive allele showed a point mutation that modifies an amino acid (Y719C) located at the beginning of the PH domain (our unpublished data).

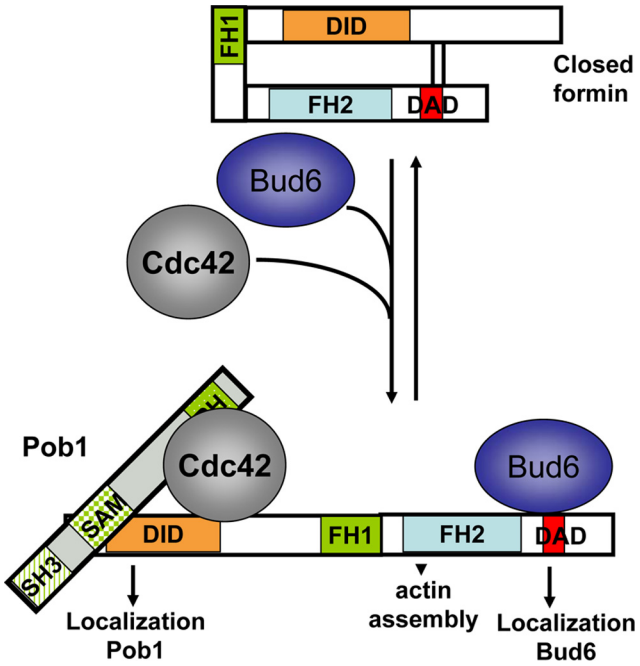

Figure 9. Model for For3 localization and activation at the cell tips. Pob1 localizes to cell tips by binding to GTP-Cdc42, and in turn serves as a tether for For3 N terminus and facilitates the Cdc42-mediated relief of For3 autoinhibition. Bud6 binding at the C terminus of For3 similarly serves as both anchor and activator of the formin (Martin *et al*., 2007).

Pob1 Regulation of the Formin For3 Localization and Autoinhibition

One important previously described effector of Cdc42 is the formin For3, necessary for actin cable formation (Martin *et al*., 2007). *cdc42-879* mutant cells show For3 localization and actin cable defects, which are partially restored upon Pob1 overproduction. No enzymatic activity has been described for the Boi proteins. Instead they contain several interaction domains with other proteins or with membranes (Bender *et al*., 1996; Hallett *et al*., 2002). We also showed that Pob1 binds For3. Therefore, we suggest that Pob1 might function facilitating the interaction of GTP-Cdc42 with other effectors like For3. According to this model (Figure 9), Pob1 would localize to the cell tips by binding to GTP-Cdc42, and in turn would help For3 to localize and facilitates the Cdc42-mediated For3 activation. Thus, the inability of the Cdc42-879–mutated protein to effectively activate For3 and promote actin cable formation may be due to its failure to bind Pob1. In agreement with this model, we found that For3 likely functions downstream of Pob1 as it is dispensable for Pob1 localization (data not shown). It had also been shown that Pob1 localizes correctly in the presence of latrunculin A (Toya *et al*., 1999). Our model is also supported by the fact that mutations in Pob1 that abolish either Cdc42 or For3 binding (*pob1-664*, *pob1ΔN*, and *pob1ΔSAM*) show similar defective actin cables and delocalized For3 phenotypes, suggesting that Pob1 forms a functional link between Cdc42 and For3.

Pob1 may regulate For3 in multiple ways. Like many formins, For3 is regulated by an autoinhibitory intramolecular interaction between its N-terminal DID domain and a C-terminal DAD sequence. Relief of this autoinhibition is regulated by Cdc42 binding at the N terminus and Bud6 binding at the C terminus (Martin *et al*., 2007). Constitutively active For3DAD* improved cell shape and partially restored actin cables, actin patch, and formin localization in *pob1* mutant strains, an effect similar to that observed in *cdc42* and *bud6Δ* mutants. This thus suggests that Pob1 contributes to relief of For3 autoinhibition. Because both Cdc42 and Pob1 bind to the N-terminal DID domain-containing fragment of For3, one possibility is that GTP-Cdc42 recruits Pob1 to compete with For3DAD binding. Alternatively, Pob1 may facilitate GTP-Cdc42 binding and competition with the DAD. Future biochemical experiment should clarify the mechanistic details of For3 relief of autoinhibition.

Pob1 also seems to function as one of the cortical tethers that localize For3 to the cell tips. For3 docking at cell tips relies on two independent localization domains—at the N and C termini. For3 C-terminal localization depends on Bud6 (Martin *et al*., 2007). We now show that localization of an N-terminal fragment of For3 is largely disrupted in *pob1ΔN* mutants, suggesting that Pob1 serves as a tether for For3 N terminus. Therefore, localization of full-length constitutively active For3 in *pob1* mutants may largely depend on the second Bud6-dependent localization domain at the C terminus. In support of this idea, we found that, in the absence of *bud6*, the *for3DAD** mutation largely fails to rescue the poor growth phenotype of *pob1ΔN* mutants (our unpublished data). Pob1 and Bud6 may thus play largely symmetric roles as both anchors and activators of For3, binding the N and C terminus of the formin, respectively.

Other Potential Roles for Pob1

It is important to note that Pob1, like Cdc42, probably plays additional roles to that of For3 regulation, because Pob1 is an essential protein and For3 is not. One tempting possibility is that Pob1 may function as an effector in other Cdc42-dependent processes essential for cell growth. For example, we observed an apparent increase in the number of patches in *cdc42-879* and *pob1* mutant strains. Although it is possible that this increase represents a side effect of formin defects, tipping the balance of F-actin toward arp2/3-dependent structures (Gao and Bretscher, 2008), it could also be possible that Pob1–Cdc42 complex regulates directly actin patch biogenesis. Pob1 may also be involved in Cdc42-dependent regulation of exocytosis, as described in *S. cerevisiae* (Wu *et al*., 2008). This would provide an interesting point of coordination between actin cable assembly and polarized vesicle delivery. Additional studies are necessary for elucidating new effectors of the Cdc42–Pob1 complex.

ACKNOWLEDGMENTS

We thank H. Valdivieso and J. C. Ribas for useful comments, M. Yamamoto for generous gifts of *pob1-664* mutant strain and *pob1*$^+$ plasmids; C. Castro for technical help with the microscopy, and D. Posner for language revision. This work was supported by grant BFU2007-60675 from the Dirección General de Investigación, MICINN, Spain, and grants SA078A07 and GR231 from Junta de Castilla y León. Work in the laboratory of S.G.M. is supported by a Swiss National Science Foundation Professorship grant (PP00A-114936) and a Human Science Program Career Development Award (CDA0016/2008).

REFERENCES

Arellano, M., Durán, A., and Pérez, P. (1997). Localization of the *Schizosaccharomyces pombe* rho1 GTPase and its involvement in the organization of the actin cytoskeleton. J. Cell Sci. *110*, 2547–2555.

Arellano, M., Valdivieso, M. H., Calonge, T. M., Coll, P. M., Durán, A., and Pérez, P. (1999). *Schizosaccharomyces pombe* protein kinase C homologues, pck1p and pck2p, are targets of rho1p and rho2p and differentially regulate cell integrity. J. Cell Sci. *112*, 3569–3578.

Bähler, J., Wu, J.-Q., Longtine, M. S., Shah, N. G., McKenzie, III, A., Steever, A. B., Wach, A., Philippsen, P., and Pringle, J. R. (1998). Heterologous mod-

ules for efficient and versatile PCR-based gene targeting in *Schizosaccharomyces pombe*. Yeast *14*, 943–951.

Bender, L., Lo, H. S., Kokojan, V., Peterson, J., and Bender, A. (1996). Associations among PH and SH3 domain-containing proteins and Rho-type GTPases in yeast. J. Cell Biol. *133*, 879–894.

Brennwald, P., and Rossi, G. (2007). Spatial regulation of exocytosis and cell polarity: yeast as a model for animal cells. FEBS Lett. *581*, 2119–2124.

Calonge, T. M., Arellano, M., Coll, P. M., and Pérez, P. (2003). Rga5p is a specific Rho1p GTPase-activating protein that regulates cell integrity in *Schizosaccharomyces pombe*. Mol. Microbiol. *47*, 507–518.

Cerione, R. A. (2004). Cdc42, new roads to travel. Trends Cell Biol. *14*, 127–132.

Chang, E. C., Barr, M., Wang, Y., Jung, V., Xu, H. P., and Wigler, M. H. (1994). Cooperative interaction of *S. pombe* proteins required for mating and morphogenesis. Cell *79*, 131–141.

Chang, E., Bartholomeusz, G., Pimental, R., Che, J., Lai, H., Wang, L., Yang, P., and Marcus, S. (1999). Direct binding and In vivo regulation of the fission yeast p21-activated kinase shk1 by the SH3 domain protein scd2. Mol. Cell. Biol. *19*, 8066–8074.

Coll, P. M., Trillo, Y., Ametzazurra, A., and Pérez, P. (2003). Gef1p, a new guanine nucleotide exchange factor for Cdc42p, regulates polarity in *Schizosaccharomyces pombe*. Mol. Biol. Cell *14*, 313–323.

Durfee, T., Becherer, K., Chen, P.-L., Yeh, S.-H., Yang, Y., Kilburn, A. E., Lee, W.-H., and Elledge, S. J. (1993). The retinoblastoma protein associates with the protein phosphatase type 1 catalytic subunit. Genes Dev. *7*, 555–569.

Endo, M., Shirouzu, M., and Yokoyama, S. (2003). The Cdc42 binding and scaffolding activities of the fission yeast adaptor protein Scd2. J. Biol. Chem. *278*, 843–852.

Etienne-Manneville, S. (2004). Cdc42—the centre of polarity. J. Cell Sci. *117*, 1291–1300.

Faix, J., and Grosse, R. (2006). Staying in shape with formins. Dev. Cell *10*, 693–706.

Feierbach, B., and Chang, F. (2001). Roles of the fission yeast formin for3p in cell polarity, actin cable formation and symmetric cell division. Curr. Biol. 1656–1665.

Forsburg, S. L. (1993). Comparison of *Schizosaccharomyces pombe* expression systems. Nucleic Acids Res. *21*, 2955–2956.

Gao, L., and Bretscher, A. (2008). Analysis of unregulated formin activity reveals how yeast can balance F-actin assembly between different microfilament-based organizations. Mol. Biol. Cell *19*, 1474–1484.

Goode, B. L., and Eck, M. J. (2007). Mechanism and function of formins in the control of actin assembly. Annu. Rev. Biochem. *76*, 593–627.

Hall, A. (2005). Rho GTPases and the control of cell behaviour. Biochem. Soc. Trans. *33*, 891–895.

Hallett, M. A., Lo, H. S., and Bender, A. (2002). Probing the importance and potential roles of the binding of the PH-domain protein Boi1 to acidic phospholipids. BMC Cell Biol. *3*, 16.

Hayles, J., and Nurse, P. (2001). A journey into space. Nat. Rev. Mol. Cell. Biol. *2*, 647–656.

Hirota, K., Tanaka, K., Ohta, K., and Yamamoto, M. (2003). Gef1p and Scd1p, the Two GDP-GTP exchange factors for Cdc42p, form a ring structure that shrinks during cytokinesis in *Schizosaccharomyces pombe*. Mol. Biol. Cell *14*, 3617–3627.

Ito, H., Fukuda, Y., Murata, K., and Kimura, A. (1983). Transformation of intact yeast cells treated with alkali cations. J. Bacteriol. *153*, 163–168.

Knechtle, P., Wendland, J., and Philippsen, P. (2006). The SH3/PH domain protein AgBoi1/2 collaborates with the Rho-type GTPase AgRho3 to prevent nonpolar growth at hyphal tips of *Ashbya gossypii*. Eukaryot. Cell *5*, 1635–1647.

Leonhard, K., and Nurse, P. (2005). Ste20/GCK kinase Nak1/Orb3 polarizes the actin cytoskeleton in fission yeast during the cell cycle. J. Cell Sci. *118*, 1033–1044.

Levin, D. E. (2005). Cell wall integrity signaling in *Saccharomyces cerevisiae*. Microbiol. Mol. Biol. Rev. *69*, 262–291.

Manser, E., Loo, T. H., Koh, C. G., Zhao, Z. S., Chen, X. Q., Tan, L., Tan, I., Leung, T., and Lim, L. (1998). PAK kinases are directly coupled to the PIX family of nucleotide exchange factors. Mol. Cell *1*, 183–192.

Martin, S. G., McDonald, W. H., Yates, J. R., 3rd, and Chang, F. (2005). Tea4p links microtubule plus ends with the formin for3p in the establishment of cell polarity. Dev. Cell *8*, 479–491.

Martin, S. G., Rincon, S. A., Basu, R., Pérez, P., and Chang, F. (2007). Regulation of the formin for3p by cdc42p and bud6p. Mol. Biol. Cell *18*, 4155–4167.

Martin, S. G., and Berthelot-Grosjean, M. (2009). Polar gradients of the DYRK-family kinase Pom1 couple cell length with the cell cycle. Nature *459*, 852–856.

Matsui, Y., Matsui, R., R., A., and Toh-e, A. (1996). Yeast *src* homology region 3 domain-binding proteins involved in bud formation. J. Cell Biol. *133*, 865–878.

McCusker, D., Denison, C., Anderson, S., Egelhofer, T. A., Yates, J. R., 3rd, Gygi, S. P., and Kellogg, D. R. (2007). Cdk1 coordinates cell-surface growth with the cell cycle. Nat. Cell Biol. *9*, 506–515.

Merla, A., and Johnson, D. I. (2000). The Cdc42p GTPase is targeted to the site of cell division in the fission yeast *Schizosaccharomyces pombe*. Int. J. Cell Biol. *79*, 469–477.

Miller, P. J., and Johnson, D. I. (1994). Cdc42p GTPase is involved in controlling polarized cell growth in *Schizosaccharomyces pombe*. Mol. Cell. Biol. *14*, 1075–1083.

Moreno, S., Klar, A., and Nurse, P. (1991). Molecular genetic analysis of fission yeast *Schizasaccharomyces pombe*. Methods Enzymol. *194*, 795–823.

Motegi, F., Arai, R., and Mabuchi, I. (2001). Identification of two type V myosins in fission yeast, one of which functions in polarized cell growth and moves rapidly in the cell. Mol. Biol. Cell, *12*, 1367–1380.

Nakano, K., Imai, J., Arai, R., Toh, E. A., Matsui, Y., and Mabuchi, I. (2002). The small GTPase Rho3 and the diaphanous/formin For3 function in polarized cell growth in fission yeast. J. Cell Sci. *115*, 4629–4639.

Park, H. O., and Bi, E. (2007). Central roles of small GTPases in the development of cell polarity in yeast and beyond. Microbiol. Mol. Biol. Rev. *71*, 48–96.

Ridley, A. J. (2006). Rho GTPases and actin dynamics in membrane protrusions and vesicle trafficking. Trends Cell Biol. *16*, 522–529.

Sayers, L. G., Katayama, S., Nakano, K., Mellor, H., Mabuchi, I., Toda, T., and Parker, P. J. (2000). Rho-dependence of *Schizosaccharomyces pombe* Pck2. Genes Cells *5*, 17–27.

Takenawa, T., and Suetsugu, S. (2007). The WASP-WAVE protein network: connecting the membrane to the cytoskeleton. Nat. Rev. Mol. Cell Biol. *8*, 37–48.

Tatebe, H., Nakano, K., Maximo, R., and Shiozaki, K. (2008). Pom1 DYRK regulates localization of the Rga4 GAP to ensure bipolar activation of Cdc42 in fission yeast. Curr. Biol. *18*, 322–330.

Toya, M., Iino, Y., and Yamamoto, M. (1999). Fission yeast Pob1p, which is homologous to budding yeast Boi proteins and exhibit subcellular localization close to actin patches, is essential for cell elongation and separation. Mol. Biol. Cell *10*, 2745–2757.

Villar-Tajadura, M. A., Coll, P. M., Madrid, M., Cansado, J., Santos, B., and Pérez, P. (2008). Rga2 is a Rho2 GAP that regulates morphogenesis and cell integrity in. *S. pombe*. Mol. Microbiol. *70*, 867–881.

Wu, H., Rossi, G., and Brennwald, P. (2008). The ghost in the machine: small GTPases as spatial regulators of exocytosis. Trends Cell Biol. *18*, 397–404.

Yang, P., Kansra, S., Pimental, R. A., Gilbreth, M., and Marcus, S. (1998). Cloning and characterization of *shk2*, a gene encoding a novel p21-activated protein kinase from fission yeast. J. Biol. Chem. *273*, 18481–18489.

Zhao, Z. S., and Manser, E. (2005). PAK and other Rho-associated kinases effectors with surprisingly diverse mechanisms of regulation. Biochem. J. *386*, 201–214.